Author/s:
Warren, AEL;Abbott, DF;Jackson, GD;Archer, JS

Title:
Thalamocortical functional connectivity in Lennox–Gastaut syndrome is abnormally enhanced in executive-control and default-mode networks

Date:
2017-12-01

Citation:
Warren, A. E. L., Abbott, D. F., Jackson, G. D. & Archer, J. S. (2017). Thalamocortical functional connectivity in Lennox–Gastaut syndrome is abnormally enhanced in executive-control and default-mode networks. Epilepsia, 58 (12), pp.2085-2097. https://doi.org/10.1111/epi.13932.

Persistent Link:
https://hdl.handle.net/11343/293822

DR. DAVID F ABBOTT (Orcid ID : 0000-0002-7259-8238)

Article type : Full length original research paper

Thalamocortical functional connectivity in Lennox-Gastaut syndrome is abnormally enhanced in executive-control and default-mode networks

Aaron E.L. Warren[1,2], David F. Abbott[1,3], Graeme D. Jackson[1,3,4], John S. Archer[1,2,3,4]

[1]Department of Medicine, The University of Melbourne, Heidelberg, Victoria, Australia

[2]Murdoch Childrens Research Institute, Parkville, Victoria, Australia

[3]The Florey Institute of Neuroscience and Mental Health, Heidelberg, Victoria, Australia

[4]Department of Neurology, Austin Health, Heidelberg, Victoria, Australia

Contact information

Name: Aaron E.L. Warren

Address: Melbourne Brain Centre, 245 Burgundy Street, Heidelberg, VIC, 3084, Australia

Email: a.warren@brain.org.au

Phone: +61 3 9035 7110

Running title: Abnormal thalamic connectivity in LGS

Key words: Lennox-Gastaut syndrome, Thalamus, fMRI, Functional connectivity, Deep Brain Stimulation

Number of pages: 35

Abstract word count: 271

Manuscript word count: 3931

Number of references: 41

Number of figures: 4 (+ 2 supplementary figures)
Number of tables: 1 (+ 4 supplementary tables)

Supporting information: Methods S1, Table S1, Table S2, Figure S1, Table S3, Table S4, Figure S2

Abstract

Objective: To identify abnormal thalamocortical circuits in the severe epilepsy of Lennox-Gastaut syndrome (LGS) that may explain the shared electroclinical phenotype and provide potential treatment targets.

Methods: Twenty patients with a diagnosis of LGS (mean age 28.5 years) and 26 healthy controls (mean age 27.6 years) were compared using task-free functional MRI (fMRI). The

thalamus was parcellated according to functional connectivity with 10 cortical networks derived using group-level independent component analysis. For each cortical network, we assessed between-group differences in thalamic functional connectivity strength using non-parametric permutation-based tests. Anatomical locations were identified by quantifying spatial overlap with a histologically-informed thalamic MRI atlas.

Results: In both groups, posterior thalamic regions showed functional connectivity with visual, auditory, and sensorimotor networks, while anterior, medial, and dorsal thalamic regions were connected with networks of distributed association cortex (including the default-mode, anterior-salience, and executive-control networks). Four cortical networks (left and right executive-control network; ventral and dorsal default-mode network) showed significantly enhanced thalamic functional connectivity strength in patients relative to controls. Abnormal connectivity was maximal in mediodorsal and ventrolateral thalamic nuclei.

Significance: Specific thalamocortical circuits are affected in LGS. Functional connectivity is abnormally enhanced between the mediodorsal and ventrolateral thalamus and the default-mode and executive-control networks, thalamocortical circuits that normally support diverse cognitive processes. In contrast, thalamic regions connecting with primary and sensory cortical networks appear to be less affected. Our previous neuroimaging studies show that epileptic activity in LGS is expressed via the default-mode and executive-control networks. Results of the present study suggest that the mediodorsal and ventrolateral thalamus may be candidate targets for modulating abnormal network behavior underlying LGS, potentially via emerging thalamic neurostimulation therapies.

Keywords: Lennox-Gastaut syndrome, Thalamus, fMRI, Functional connectivity, Deep Brain Stimulation

Key points

- Thalamic functional connectivity with ten cortical networks was compared between healthy controls and patients with LGS using task-free fMRI

- Patients showed abnormally enhanced connectivity between the mediodorsal and ventrolateral thalamus and the executive-control and default-mode networks
- Posterior thalamic areas, which displayed connectivity with primary and sensory networks, were not significantly affected in LGS
- Specific thalamocortical circuits are involved in LGS. These results may inform emerging thalamic neurostimulation therapies for patients

Introduction

Lennox-Gastaut syndrome (LGS) is a severe epilepsy associated with multiple seizure types (including generalized tonic seizures) and intellectual impairment[1]. On interictal electroencephalography (EEG), patients have characteristic epileptiform discharges, including frequent bursts of generalized paroxysmal fast activity and slow spike-and-wave.

While causes of LGS are diverse (e.g., genetic, structural, and acquired etiologies), the electroclinical expression appears to involve shared neural systems[2]. At a cortical level, our previous studies using concurrent EEG-fMRI revealed that epileptiform discharges in LGS spatially intersect with distributed functional networks that normally support key cognitive processes, including frontal and parietal areas of the default-mode and executive-control networks[3-5]. Similar regions of association cortex show increased blood flow during tonic seizures in LGS[6], as measured by ictal single-photon emission computed tomography (SPECT).

Several lines of evidence suggest that the thalamus also participates in network dysfunction underlying refractory epilepsy and cognitive impairment in LGS. EEG-fMRI studies[3-5,7] and intracranial recordings[8] show thalamic involvement during epileptic activity, and abnormal thalamic metabolism is found on ^{18}fluorodeoxyglucose positron emission tomography (FDG-PET)[9]. Thalamic stimulation has shown some efficacy in reducing seizure frequency in patients with LGS[10], although the optimal stimulation targets remain uncertain[11].

We previously observed that patients with LGS show persistently disrupted cortico-cortical functional connectivity[12], as assessed using task-free fMRI by measuring low-frequency temporal correlations in the blood-oxygen-level-dependent signal. Specifically, we examined interactions among cortical networks known to be involved in the expression of epileptic activity in LGS[3-6], and found reduced functional connectivity within the default-mode network, and abnormally enhanced connectivity between the default-mode and executive-control networks[12]. In the healthy brain, the thalamus plays a critical role in mediating normal interactions among these cortical networks[13-15]. This raises the possibility that the thalamus may contribute to abnormal cortical functional organization in LGS.

In the present study, we used task-free fMRI to compare functional connectivity between the thalamus and 10 cortical networks in healthy controls and patients with LGS. Given our previous neuroimaging studies suggesting that multiple causes of LGS converge on specific cortical areas involved in the expression of epileptic activity[3-6,12], we hypothesized that patients with diverse underlying etiologies of LGS would show a common pattern of abnormal functional connectivity involving specific thalamocortical circuits.

Methods

Participants

Twenty-eight patients were recruited through Austin Health (Melbourne, Australia) and satisfied the following inclusion criteria: i) no prior history of neurosurgery, and ii) an electroclinical diagnosis of LGS consistent with recent consensus opinion[1], including tonic seizures, generalized slow (<3 Hz) spike-and-wave discharges on routine EEG, and generalized paroxysmal fast activity on routine EEG during sleep. Twenty-seven healthy controls with no history of neurological or psychiatric illness were also recruited. Before recruitment began, this study was approved by the Austin Health Human Research Ethics Committee. Written informed consent was given by each subject or their legal guardian.

After participation, data from 9 subjects (8 patients and 1 control) were excluded due to excessive head motion[16] or MRI artifacts. The final samples therefore comprised 20 patients with LGS (10 females; mean age±1 standard deviation [SD]=28.5±10.5 years) and 26 healthy controls (10 females; mean age=27.6±8.8 years).

Electroclinical characteristics of patients

Detailed electroclinical characteristics of each patient are provided in Table 1. The median age of seizure onset was 4.5 years, and median duration of epilepsy was 23 years. Presumed etiologies underlying epilepsy included genetic or chromosomal abnormalities (5 patients), cortical malformations (2 patients), and acquired brain pathologies (4 patients). Etiology was unknown in 9 patients. On anatomical MRI, nine patients showed potentially epileptogenic lesions (e.g., focal cortical dysplasia, peri-ventricular nodular heterotopia), while the remaining 11 patients had either normal MRI findings or structural features of uncertain significance (e.g., atrophy). Severity of cognitive impairment was variable across patients. In nine patients for whom formal clinical neuropsychological assessment was available, mild to severe intellectual disability (intelligence quotient [IQ] < 70) was observed in six patients, and borderline intellectual disability (IQ=70-80) in three. In the remaining 11 patients, variable cognitive profiles were described by each patient's treating neurologist: those with an early age of seizure onset (<4 years) were considered to have moderate or severe cognitive impairment, and were described as non-verbal or minimally verbal, while those with an older age of seizure onset experienced mild to severe cognitive impairment and/or difficulties in specific cognitive domains (e.g., deficits in working memory or verbal memory).

MRI data acquisition

Task-free fMRI data were acquired as part of a larger multi-site study of LGS[3-5,12]. All subjects were scanned using T2*-weighted gradient-recalled echo-planar image sequences (for detailed acquisition parameters, refer to Methods S1). Thirty-one subjects (15 patients and 16 controls) were scanned using a 3 tesla GE Signa LX MRI, as we have previously described[12]. A further 15 subjects (5 patients and 10 controls) were scanned using a 3 tesla Siemens Trio MRI utilizing a similar imaging protocol. 210 whole-brain fMRI volumes were available in each subject, during which they were instructed to lie still with eyes closed. To minimize potential bias introduced by the use of multi-scanner fMRI data, we included scanner type as a nuisance covariate in all statistical comparisons. A T1-weighted image also was acquired for each subject to guide spatial normalization of fMRI data.

fMRI data pre-processing and de-noising

Detailed description of fMRI pre-processing and de-noising is provided in Methods S1. Briefly, each subject's fMRI data were temporally interpolated to yield a uniform slice acquisition, spatially realigned to the middle volume in each dataset, co-registered with each subject's T1, and then warped to the Montreal Neurological Institute's (MNI)-152 T1 atlas.

De-noising steps included i) removing variance attributable to head motion and signals from white matter and cerebrospinal fluid; ii) removing the effect of volumes affected by gross head motion ("scrubbing") by including a regressor for each volume with frame-wise displacement exceeding 0.5 mm, and also for the following two volumes[16]; iii) temporal frequency filtering (0.01-0.1 Hz); and iv) deleting scrubbed volumes. De-noised data were spatially smoothed using a Gaussian kernel with full-width-at-half-maximum=4 mm.

After de-noising, residual head motion (i.e., each subject's mean frame-wise displacement after removal of scrubbed fMRI data) was significantly different between groups (mean±1 SD in LGS=0.15±0.05 mm; controls=0.12±0.04 mm; two-sample *t*-test $p=0.02$). To minimize potential bias caused by these subtle motion differences, residual head motion was included as a nuisance covariate in all statistical comparisons.

Cortical networks of interest

Cortical networks were defined using group-level independent component analysis (ICA). Twenty-five components were estimated from the temporally concatenated de-noised fMRI data of all subjects using the Infomax algorithm available in the Group ICA of fMRI Toolbox (http://mialab.mrn.org/software/gift). For each component, subject-specific spatial maps were derived using group-information-guided ICA[17]. Results were converted to *z*-scores and then averaged across all subjects. Ten average spatial maps were selected as cortical networks of interest (Figure 1B) by identifying components showing high spatial correlation ($r>0.3$) with established cortical network templates[18]. Finally, non-overlapping cortical network masks were defined by first thresholding average spatial maps at $z>1.5$, and then assigning each surviving voxel to the component with the highest mean *z*-score at that voxel. Anatomical locations encompassed by each cortical network mask are described in Table S1.

Thalamocortical functional connectivity

A thalamic mask was defined using the Harvard-Oxford subcortical atlas (http://fsl.fmrib.ox.ac.uk/fsl/fslwiki/Atlases). To avoid partial inclusion of neighboring ventricles, voxels classified as cerebrospinal fluid on subjects' T1 images were excluded. Functional connectivity was then calculated using the Fisher's *r*-to-*z* transformed Pearson correlation between the time-series of each thalamic voxel, and the principal component time-series across all voxels within each cortical network mask[14]. The principal component was calculated using Analysis of Functional NeuroImage's (AFNI's) *3dmaskSVD* function (https://afni.nimh.nih.gov/pub/dist/doc/program_help/3dmaskSVD.html).

Winner-takes-all thalamic parcellation

For LGS and control groups separately, a winner-takes-all approach[19] was used to parcellate the thalamus based on territories of 'dominant' functional connectivity occupied by each cortical network. This involved assigning each thalamic voxel to the cortical network with the strongest mean functional connectivity at that voxel. To assess consistency of thalamic parcellations, we used a bootstrapping strategy[13,20] whereby 10,000 random samplings (with replacement) were separately performed within each group. For each resulting sample, a winner-takes-all map was generated from the corresponding mean thalamocortical connectivity values. Finally, each thalamic voxel was labelled according to the mode of all winner-takes-all assignments across the 10,000 bootstrapped samples. Consistency was thus evaluated as the proportion of assignments equal to the mode[13].

Strength of thalamocortical functional connectivity

Winner-takes-all parcellation can obscure thalamic regions showing significant connectivity with multiple cortical areas[19], and may underestimate differences in relative connectivity strength[14]. For each cortical network, we therefore explored i) thalamic regions showing significantly positive connectivity, computed separately for LGS and control groups; and ii) thalamic regions showing significant between-group differences in connectivity strength. Note that these analyses examined functional connectivity between each thalamic voxel and each cortical network (i.e., the winner-takes-all thalamic parcellations obtained in the previous step were not used to calculate thalamocortical functional connectivity here).

A one-sample *t*-test design was used to assess significance of thalamocortical connectivity strength within each group, and a two-sample *t*-test design was used to assess significance of differences in thalamocortical connectivity strength between groups. Analyses were implemented in FMRIB Software Library's (FSL's) *randomise* function[21], a non-parametric permutation-based inference tool (10,000 permutations were performed for each analysis). Threshold-free cluster enhancement[21] was used for statistical inference, with significance assessed at a voxel-wise threshold of $p<0.05$ (corrected for family-wise error). Each analysis was adjusted using nuisance covariates for age, sex, scanner type, and residual head motion.

Additional exploratory analyses were performed for the subset of cortical networks showing significant between-group differences in thalamocortical connectivity strength. To test whether similar patterns of abnormal connectivity were present in patients with and without presumed epileptogenic lesions evident on anatomical MRI, we separately compared the sub-group of nine patients with lesions (patient #s 1, 6, 8, 9, 10, 11, 13, 14, and 20 in Table 1) and the sub-group of 11 patients without lesions (patient #s 2, 3, 4, 5, 7, 12, 15, 16, 17, 18, and 19 in Table 1) to the group of healthy controls (n=26). These between-group analyses were performed using FSL's *randomise* function[21], as described above. Noting the small sample size in each of the patient sub-groups, significance was assessed at an exploratory voxel-wise threshold of $p<0.025$ (uncorrected) following threshold-free cluster enhancement[21].

Association with age of seizure onset

For each cortical network, we assessed the effect of seizure onset age (in years) on thalamocortical connectivity strength in the patient group using linear regression in FSL's *randomise* (10,000 permutations)[21], adjusting for age, sex, scanner type, and residual head motion. Threshold-free cluster enhancement[21] was applied for statistical inference, with significance assessed at a voxel-wise threshold of $p<0.05$ (corrected for family-wise error).

Spatial overlap with histologically-informed thalamic MRI atlas

To assist with identification of thalamic nuclear groups involved in our functional connectivity analyses, we calculated spatial overlap with a 3-dimensional MRI atlas derived from human thalamic histology[22]. This atlas comprises binary masks of approximately 40 thalamic structures at high voxel resolution (0.5 mm^3) available in standard MNI space. For

the present analyses, select structures were combined into 9 distinct nuclear groups in accordance with known thalamic cytoarchitecture[22] (for details concerning how thalamic structures were combined, refer to Table S2). Binary masks of each thalamic nuclear group were down-sampled to 2 mm^3 to match the resolution of our fMRI analyses. Overlap was then quantified via the Dice coefficient, a measure of spatial similarity between binary image pairs (for detailed description, refer to Methods S1).

Results

Winner-takes-all thalamic parcellation

In both LGS and control groups, winner-takes-all thalamic parcellation revealed a generally symmetrical representation of thalamic areas assigned to bilateral cortical networks (Figure 1A). To facilitate identification of thalamic territories, spatial overlap with the thalamic atlas[22] is quantified using Dice coefficients in Table S3. Overall, high consistency was observed for the bootstrapped parcellations. Median consistency of thalamic voxel assignments across 10,000 bootstrapped samples was 77% in controls and 70% in LGS (Figure S1).

In both groups, posterior thalamus (including pulvinar, posterior intralaminar, and ventroposterior nuclei) showed dominant functional connectivity with primary and sensory networks (visual, sensorimotor, and auditory), while anterior, medial, and dorsal thalamus (including anterior, mediodorsal, and medial pulvinar nuclei) were mainly assigned to networks of association and limbic cortex (anterior-salience, dorsal default-mode, and executive-control). In both groups, the anterior-salience and sensorimotor networks occupied the largest thalamic territories; each network showed strongest connectivity with >20% of all thalamic voxels (Figure 1C). In contrast, the dorsal-attention, posterior-salience, and ventral default-mode networks showed little or no dominant territory.

On visual inspection, LGS patients showed increased dominant thalamic territory for the left and right executive-control networks (Figures 1A and 1C). Specifically, compared to controls, a greater proportion of voxels including left and right anterior and ventrolateral nuclei showed strongest connectivity with the left and right executive-control networks,

respectively; in controls, these nuclei instead showed dominant connectivity with the anterior-salience or dorsal default-mode networks.

Thalamocortical functional connectivity strength in each group

In each group, analysis of functional connectivity strength (Figure 2) revealed more extensive patterns of thalamocortical connectivity than found by the winner-takes-all parcellation. For each result, spatial overlap with the thalamic atlas[22] is quantified using Dice coefficients in Table S4.

Several thalamic regions showed significant connectivity strength with multiple cortical networks. In both LGS and control groups, the visual, sensorimotor, and auditory networks showed overlapping connectivity with the pulvinar, ventroposterior, and posterior intralaminar nuclei. Additionally, cortical networks thought to support related functional roles displayed similar patterns of thalamic connectivity. For example, dorsal and ventral components of the default-mode network each displayed bilateral connectivity with the medial region of the pulvinar, while the left and right executive-control networks showed similar connectivity with the anterior thalamus.

On visual inspection, networks encompassing prefrontal, parietal, and temporal cortex displayed more diffuse patterns of thalamic connectivity in LGS relative to controls. Specifically, patients showed more extensive connectivity between the mediodorsal and ventrolateral thalamus and i) the right and left executive-control networks, and ii) the dorsal and ventral default-mode networks.

Abnormally enhanced thalamocortical functional connectivity strength in LGS

Four networks showed significantly increased thalamocortical connectivity strength ($p<0.05$, family-wise error corrected) in patients relative to controls (Figure 3). Patients showed enhanced bilateral thalamic connectivity with the left and right executive-control networks, and the ventral default-mode network. Spatial overlap with the thalamic atlas[22] indicated that these connectivity increases were maximal in the mediodorsal and ventrolateral thalamus. Enhanced connectivity was also observed between the dorsal default-mode network and a

small area of the left thalamus involving ventromedial and ventral anterior nuclei. No areas of reduced connectivity were observed in patients relative to controls.

To visualize thalamic areas in patients showing abnormal connectivity with multiple cortical networks, we computed a summary map by i) binarizing and then summing all significant thalamic voxels (p<0.05) from each between-group comparison, and ii) applying a threshold of >1. The resulting summary map showed maximal participation of the mediodorsal and ventrolateral thalamus (Figure 4).

Abnormally enhanced thalamocortical functional connectivity strength in lesional and non-lesional LGS sub-groups

Figure S2 displays results of the exploratory analyses comparing each of two patient sub-groups (i.e., patients with presumed epileptogenic lesions evident on anatomical MRI, and patients without such lesions) against healthy controls. In both patient sub-groups, abnormal connectivity was similar to that seen at the whole-group level, including enhanced connectivity between i) the thalamus and the dorsal and ventral default-mode networks; and ii) the thalamus and the left and right executive-control networks (Figure S2). In both sub-groups, no areas of reduced connectivity were observed in patients relative to controls.

Association with age of seizure onset

In patients, no cortical network showed a significant linear relationship between seizure onset age and thalamic functional connectivity strength (all p>0.13, family-wise error corrected).

Discussion

Specific thalamocortical circuits are affected in LGS. Functional connectivity is abnormally enhanced between the mediodorsal and ventrolateral thalamus and the cortical executive-control and default-mode networks. In contrast, posterior thalamic regions, which show dominant connectivity with primary and sensory cortical networks, appear to be less affected. Furthermore, patterns of abnormal thalamocortical functional connectivity in LGS are observable in patient sub-groups with and without presumed epileptogenic lesions evident on anatomical MRI, adding further evidence to support the hypothesis that the shared

electroclinical features of LGS reflect a 'secondary network epilepsy'[2,4], in which abnormal epileptic behavior is expressed across a shared network, rather than reflecting the specific lesional or non-lesional etiology.

Previous fMRI studies in healthy subjects[19,23] and epilepsy patients[20] have parcellated the thalamus by measuring connectivity with anatomically-defined cortical lobes. Here we show that the thalamus can also be parcellated according to *functional* cortical network organization, adding to prior evidence in healthy subjects[13-15] and extending the clinical utility of this approach. Given the growing understanding of epilepsy as a disorder of large-scale functional systems that often involve distributed brain areas[12], we suggest that the use of functionally-defined cortical network regions-of-interest is well-suited to explore clinically relevant markers of thalamocortical dysfunction, and may reveal new treatment targets.

We speculate that abnormal thalamic interactions with the executive-control and default-mode networks may contribute to cognitive deficits typically observed in LGS. The affected networks comprise distributed areas of prefrontal, parietal, and temporal cortex that normally support a broad range of cognitive functions[13,18]. Prior fMRI studies show that abnormal thalamus-default-mode connectivity is associated with impaired intellect in severe childhood epilepsy[24], while aberrant thalamus-executive-control connectivity is linked to deficits in working memory and verbal learning[25]. We previously found that widespread areas of the executive-control and default-mode networks are recruited during tonic seizures[6] and epileptiform discharges[3-5] in LGS. Additionally, LGS patients show abnormal functional connectivity within the default-mode network, and between the default-mode and executive-control networks[5,12]. Considered together, these results raise the hypothesis that the expression of epileptic activity in thalamus-executive-control and thalamus-default-mode circuits disrupts normal connectivity, potentially contributing to impaired cognition in LGS.

Pathology of the mediodorsal and ventrolateral thalamus has previously been associated with several electroclinical features of LGS. Early ischemic injuries to the mediodorsal or ventrolateral thalamus can lead to epileptic encephalopathy, with patients developing tonic and other generalized seizures, interictal slow spike-and-wave, and developmental regression[26]. Ictal SPECT studies show hyper-perfusion of the mediodorsal nucleus during secondarily generalized tonic-clonic convulsions[27] as well as gelastic seizures in patients with hypothalamic hamartoma[28], an epilepsy that often evolves to a Lennox-Gastaut phenotype.

Furthermore, in rodent models of generalized absence epilepsy, kainic acid injections to the mediodorsal nucleus elicit slow spike-and-wave[29], bilateral removal of the mediodorsal nucleus abolishes slow spike-and-wave[30], and genetically predisposed strains develop spontaneous absence seizures that show early involvement of the ventrolateral thalamus[31].

Our findings in LGS show notable differences to previous observations in other generalized epilepsy syndromes. Relative to healthy controls, patients with genetic generalized epilepsy (GGE) show *reduced* functional connectivity between the mediodorsal thalamus and prefrontal/parietal areas of the default-mode network[32,33]. These thalamocortical circuits spatially overlap with those found here to be affected in LGS, however the expression of abnormal activity appears to differ (i.e., *reduced* thalamocortical connectivity in GGE; *enhanced* thalamocortical connectivity in LGS). Consistent with this observation, EEG-fMRI studies of epileptiform discharges in GGE and LGS show divergent patterns of fMRI signal change in brain networks involved in both syndromes (e.g., *deactivation* of the default-mode network during generalized spike-and-wave in GGE[34]; *activation* of the default-mode network during generalized paroxysmal fast activity in LGS[3-5]). These functional differences may help to explain the distinct electroclinical profiles of these epilepsy syndromes.

The thalamocortical circuits affected in LGS include brain areas with known vulnerability to maturational dysregulation. For example, thalamic functional connectivity with prefrontal areas of the default-mode and executive-control networks is significantly refined throughout childhood and adolescence[13,23], increasing the susceptibility of these circuits to developmental insults[14]. Similarly, in immature rodents, lithium-pilocarpine-induced status epilepticus preferentially damages the mediodorsal thalamus[35,36], and an earlier age at seizure onset is associated with more severe mediodorsal injury[36], greater cognitive impairment in later life[37], and enhanced likelihood of epileptogenesis[37]. Given that the patients in our study developed seizures in parallel with these critical neurodevelopmental periods, one possibility is that LGS induces an altered trajectory of thalamocortical maturation. This would be consistent with prior studies showing that intractable childhood epilepsy interferes with functional connectivity development of the thalamus and default-mode network[5,24,38].

Furthermore, thalamocortical circuits that appear to be *less* affected in LGS include brain areas with several developmental advantages that may protect against early life insults. We found that LGS patients and controls showed similar connectivity between posterior thalamic

regions (including ventroposterior and pulvinar nuclei) and the visual, auditory, and sensorimotor networks. These primary and sensory systems are among the first thalamocortical circuits to emerge during pre-natal functional connectivity development[39], and their maturation occurs earlier than higher-order networks of association cortex, such as the default-mode and executive-control networks[13,23]. We speculate that this earlier developmental window may reduce the vulnerability of primary and sensory systems to potential impacts of LGS on thalamocortical maturation. Consistent with this hypothesis, some patients with LGS show a relative preservation of motor functions compared to patients with other epileptic encephalopathies[40]. Additionally, abnormal metabolism on FDG-PET typically spares primary cortex in LGS[2], while ictal SPECT[6] and interictal EEG-fMRI[3-5] studies show reduced involvement of primary cortical areas during epileptic activity.

Identification of thalamocortical circuits maximally affected in LGS may have implications for emerging neurostimulation treatments. Although therapeutic mechanisms remain unclear, efficacy of thalamic stimulation for epilepsy is likely maximized when stimulation is tailored to the specific thalamocortical circuits underlying seizures. For example, stimulation of the anterior nucleus of the thalamus, which projects strongly to temporal cortex and the limbic system, shows effectiveness in temporal lobe epilepsy[41], but benefits are less apparent for seizures of extra-temporal origin[41]. In LGS, interest in thalamic stimulation has largely focused on the centromedian nucleus, a sub-division of the posterior intralaminar complex that is thought to modulate diffuse cortical activity via widespread, non-specific interactions with superficial cortical layers[10,11]. In the present study we show that LGS affects specific functional interactions between the mediodorsal and ventrolateral thalamus and the cortical executive-control and default-mode networks, a finding that aligns with previous SPECT[6], EEG-fMRI[3-5], and FDG-PET[2,9] studies showing that epileptic activity in LGS is expressed via these circuits. Taken together, our results suggest that network-tailored stimulation, potentially targeting the mediodorsal or ventrolateral thalamus, may be a candidate therapeutic strategy to explore further in LGS.

Limitations and future directions

The clinical utility of these findings requires additional investigation. Although we show that abnormal connectivity in LGS affects specific thalamocortical circuits that normally support key cognitive functions[13,18], further studies are needed to determine a more detailed

association between altered connectivity and neuropsychological outcomes in LGS. Potential effects of anti-epileptic medications on our results cannot be excluded. While it is possible our results were influenced by patients' in-scanner epileptiform discharges, we previously observed that abnormal functional connectivity in LGS persists during fMRI periods without scalp EEG-recorded discharges[12], suggesting that enhanced connectivity may reflect a more pervasive configuration of affected circuits. Finally, we note that a small number of patients included in our study had a seizure onset age considered less typical for LGS (>9 years; Table 1). However, across our patient group we did not find a significant association between thalamocortical functional connectivity and age of seizure onset, suggesting that the shared electroclinical phenotype may better explain our observed patterns of abnormal connectivity.

Conclusions

Our findings identify specific thalamocortical circuits affected in Lennox-Gastaut syndrome (LGS). Despite heterogeneous etiologies, functional connectivity is abnormally enhanced between the mediodorsal and ventrolateral thalamus, and the cortical default-mode and executive-control networks. In contrast, posterior thalamic areas, which show dominant connectivity with primary and sensory cortical networks, are less affected in LGS. Given our previous studies showing that epileptic activity in LGS disrupts the default-mode and executive-control networks[3-6,12], we hypothesize that the mediodorsal and ventrolateral thalamus may be candidate targets for modulating abnormal network behavior underlying LGS, potentially via emerging thalamic neurostimulation therapies.

Acknowledgements

We thank the patients and their families for participating in this research. We also thank Shawna Farquharson and the Florey radiography team for MRI scanning, Dr Neelan Pillay for contributions to patient recruitment, and Professor Sam Berkovic for manuscript advice. This study was supported by the National Health and Medical Research Council of Australia, project grant 628725 (John S. Archer and David F. Abbott), and practitioner fellowship 1060312 (Graeme D. Jackson). Aaron E.L. Warren is supported by an Australian Government Research Training Program Scholarship, and fellowship funding from the Lennox-Gastaut syndrome Foundation (LGS Foundation). David F. Abbott is supported by fellowship funding from the National Imaging Facility. We acknowledge the facilities and the

scientific and technical assistance of the National Imaging Facility at the Florey node, and the support of the Victorian Government through the Operational Infrastructure Support Grant.

Disclosure of conflicts of interest

None of the authors has any conflict of interest relevant to this research activity to disclose. We confirm that we have read the Journal's position on issues involved in ethical publishing and affirm that this report is consistent with those guidelines.

References

1. Arzimanoglou A, French J, Blume WT, et al. Lennox-Gastaut syndrome: a consensus approach on diagnosis, assessment, management, and trial methodology. Lancet Neurol 2009; 8: 82-93.
2. Archer JS, Warren AEL, Jackson GD, et al. Conceptualising Lennox-Gastaut Syndrome as a secondary network epilepsy. Front Neurol 2014; 5: 1-11.
3. Pillay N, Archer JS, Badawy RA, et al. Networks underlying paroxysmal fast activity and slow spike and wave in Lennox-Gastaut syndrome. Neurology 2013; 81: 665-673.
4. Archer JS, Warren AEL, Stagnitti MR, et al. Lennox-Gastaut Syndrome and Phenotype: secondary network epilepsies. Epilepsia 2014; 55: 1245-1254.
5. Warren AEL, Harvey AS, Abbott DF, et al. Cognitive network reorganization following surgical control of seizures in Lennox-Gastaut syndrome. Epilepsia (in press 2017).
6. Intusoma U, Abbott DF, Masterton RA, et al. Tonic seizures of Lennox-Gastaut syndrome: periictal single-photon emission computed tomography suggests a corticopontine network. Epilepsia 2013; 54: 2151-2157.

7. Siniatchkin M, Coropceanu D, Moeller F, et al. EEG-fMRI reveals activation of brainstem and thalamus in patients with Lennox-Gastaut syndrome. Epilepsia 2011; 52: 766-774.
8. Velasco M, Velasco F, Alcalá H, et al. Epileptiform EEG activity of the centromedian thalamic nuclei in children with intractable generalized seizures of the Lennox-Gastaut syndrome. Epilepsia 1991; 32: 310-321.
9. Ferrie C, Marsden P, Maisey M, et al. Cortical and subcortical glucose metabolism in childhood epileptic encephalopathies. J Neurol Neurosurg Psychiatry 1997; 63: 181-187.
10. Velasco AL, Velasco F, Jiménez F, et al. Neuromodulation of the centromedian thalamic nuclei in the treatment of generalized seizures and the improvement of the quality of life in patients with Lennox–Gastaut syndrome. Epilepsia 2006; 47: 1203-1212.
11. Fisher RS, Uematsu S, Krauss GL, et al. Placebo-controlled pilot study of centromedian thalamic stimulation in treatment of intractable seizures. Epilepsia 1992; 33: 841-851.
12. Warren AEL, Abbott DF, Vaughan DN, et al. Abnormal cognitive network interactions in Lennox-Gastaut syndrome: a potential mechanism of epileptic encephalopathy. Epilepsia 2016; 57: 812-822.
13. Alcauter S, Lin W, Smith JK, et al. Development of thalamocortical connectivity during infancy and its cognitive correlations. J Neurosci 2014; 34: 9067-9075.
14. Toulmin H, Beckmann CF, O'Muircheartaigh J, et al. Specialization and integration of functional thalamocortical connectivity in the human infant. Proc Natl Acad Sci U S A 2015; 112: 6485-6490.
15. Yuan R, Di X, Taylor PA, et al. Functional topography of the thalamocortical system in human. Brain Struct Funct 2016; 221: 1971-1984.
16. Power JD, Barnes KA, Snyder AZ, et al. Spurious but systematic correlations in functional connectivity MRI networks arise from subject motion. Neuroimage 2012; 59: 2142-2154.
17. Du Y, Fan Y. Group information guided ICA for fMRI data analysis. Neuroimage 2013; 69: 157-197.
18. Yeo BT, Krienen FM, Sepulcre J, et al. The organization of the human cerebral cortex estimated by intrinsic functional connectivity. J Neurophysiol 2011; 106: 1125-1165.
19. Zhang D, Snyder AZ, Fox MD, et al. Intrinsic functional relations between human cerebral cortex and thalamus. J Neurophysiol 2008; 100: 1740-1748.

20. He X, Doucet GE, Sperling M, et al. Reduced thalamocortical functional connectivity in temporal lobe epilepsy. Epilepsia 2015; 56: 1571-1579.
21. Winkler AM, Ridgway GR, Webster MA, et al. Permutation inference for the general linear model. Neuroimage 2014; 92: 381-397.
22. Krauth A, Blanc R, Poveda A, et al. A mean three-dimensional atlas of the human thalamus: generation from multiple histological data. Neuroimage 2010; 49: 2053-2062.
23. Fair DA, Bathula D, Mills KL, et al. Maturing thalamocortical functional connectivity across development. Front Syst Neurosci 2010; 4: 10.
24. Ibrahim GM, Morgan BR, Smith ML, et al. Thalamocortical connectivity is enhanced following functional hemispherotomy for intractable lateralized epilepsy. Epilepsy Behav 2015; 51: 281-285.
25. Woodward ND, Heckers S. Mapping thalamocortical functional connectivity in chronic and early stages of psychotic disorders. Biol Psychiatry 2016; 79: 1016-1025.
26. Guzzetta F, Battaglia D, Veredice C, et al. Early thalamic injury associated with epilepsy and continuous spike–wave during slow sleep. Epilepsia 2005; 46: 889-900.
27. Blumenfeld H, Varghese G, Purcaro M, et al. Cortical and subcortical networks in human secondarily generalized tonic-clonic seizures. Brain 2009; 132: 999-1012.
28. Kameyama S, Masuda H, Murakami H. Ictogenesis and symptomatogenesis of gelastic seizures in hypothalamic hamartomas: an ictal SPECT study. Epilepsia 2010; 51: 2270-2279.
29. Kato K, Urino T, Hori T, et al. Experimental petit mal-like seizure induced by microinjection of kainic acid into the unilateral mediodorsal nucleus of the thalamus. Neurol Med Chir (Tokyo) 2008; 48: 285-291.
30. Banerjee PK, Snead OC. Thalamic mediodorsal and intralaminar nuclear lesions disrupt the generation of experimentally induced generalized absence-like seizures in rats. Epilepsy Res 1994; 17: 193-205.
31. Vergnes M, Marescaux C, Depaulis A. Mapping of spontaneous spike and wave discharges in Wistar rats with genetic generalized non-convulsive epilepsy. Brain Res 1990; 523: 87-91.
32. Wang Z, Zhang Z, Jiao Q, et al. Impairments of thalamic nuclei in idiopathic generalized epilepsy revealed by a study combining morphological and functional connectivity MRI. PLoS One 2012; 7: e39701.
33. Kim JB, Suh SI, Seo WK, et al. Altered thalamocortical functional connectivity in idiopathic generalized epilepsy. Epilepsia 2014; 55: 592-600.

34. Carney PW, Masterton RA, Harvey AS, et al. The core network in absence epilepsy. Differences in cortical and thalamic BOLD response. Neurology 2010; 75: 904-911.
35. Kubová H, Druga R, Lukasiuk K, et al. Status epilepticus causes necrotic damage in the mediodorsal nucleus of the thalamus in immature rats. J Neurosci 2001; 21: 3593-3599.
36. Kubová H, Druga R, Haugvicová R, et al. Dynamic changes of status epilepticus-induced neuronal degeneration in the mediodorsal nucleus of the thalamus during postnatal development of the rat. Epilepsia 2002; 43: 54-60.
37. Kubová H, Mares P, Suchomelová L, et al. Status epilepticus in immature rats leads to behavioural and cognitive impairment and epileptogenesis. Eur J Neurosci 2004; 19: 3255-3265.
38. Ibrahim GM, Morgan BR, Lee W, et al. Impaired development of intrinsic connectivity networks in children with medically intractable localization-related epilepsy. Hum Brain Mapp 2014; 35: 5686-5700.
39. Doria V, Beckmann CF, Arichi T, et al. Emergence of resting state networks in the preterm human brain. Proc Natl Acad Sci U S A 2010; 107: 20015-20020.
40. Aljaafari D, Fasano A, Nascimento FA, et al. Adult motor phenotype differentiates Dravet syndrome from Lennox-Gastaut syndrome and links SCN1A to early onset parkinsonian features. Epilepsia 2017; 58: e44-e48.
41. Fisher R, Salanova V, Witt T, et al. Electrical stimulation of the anterior nucleus of thalamus for treatment of refractory epilepsy. Epilepsia 2010; 51: 899-908.

Figure legends

Figure 1 : Winner-takes-all thalamic parcellation using 10 cortical networks of interest
A) In LGS and control groups separately, each thalamic voxel was assigned to the cortical network representing the most frequent assignment across 10,000 bootstrapped samples (for each sample, each thalamic voxel was assigned to the cortical network with the strongest mean functional connectivity at that voxel). Thalamic voxel colors match the cortical network masks shown in Figure 1B. Results are displayed on the MNI-152 T1 brain template. The *z* coordinate on each thalamic image indicates the axial position in MNI space. To facilitate identification of thalamic regions participating in each result, spatial overlap with a histologically-informed thalamic MRI atlas[22] is quantified (Dice coefficients) in Table S3.
B) Binary masks of 10 cortical networks derived from the temporally concatenated fMRI data of all subjects (healthy controls and LGS patients together) using group-level independent component analysis (ICA). Anatomical locations encompassed by each cortical network are listed in Table S1. Cortical network abbreviations: VIS=visual; SM=sensorimotor; AUD=auditory; DAN=dorsal-attention network; pSN=posterior-salience network; aSN=anterior-salience network; RECN=right executive-control network; LECN=left executive-control network; dDMN=dorsal default-mode network; vDMN=ventral default-mode network.
C) For each group, the spatial extent of each cortical network's dominant thalamic territory (i.e., the proportion of thalamic voxels assigned to each cortical network in the winner-takes-all parcellations seen in Figure 1A). Cortical network abbreviations are as per Figure 1B.

Figure 2 : Within-group analysis of thalamocortical functional connectivity strength
Thalamic regions showing significantly positive functional connectivity strength ($p<0.05$, 10,000 permutations, corrected for family-wise error following threshold-free cluster enhancement[21]) with each cortical network. Results are displayed separately for healthy control and LGS groups. The color of each cortical network matches its area of significant thalamic connectivity. Results are displayed on the MNI-152 T1 brain template. The *z*

coordinate displayed on each thalamic image indicates the axial position in MNI space. Cortical network abbreviations are as per Figure 1B. To facilitate identification of thalamic regions participating in each result, spatial overlap with a histologically-informed thalamic MRI atlas[22] is quantified (Dice coefficients) in Table S4.

Figure 3 : Significantly enhanced thalamocortical functional connectivity strength in LGS

Left: Cortical networks and thalamic regions showing significantly enhanced functional connectivity strength in patients relative to healthy controls ($p<0.05$, 10,000 permutations, corrected for family-wise error following threshold-free cluster enhancement[21]). Results are colored using *p* values, where hotter (more yellow) areas indicate more significant voxels (i.e., values closer to zero). Results are displayed on the MNI-152 T1 brain template. The *z* and *x* coordinates on thalamic images indicate axial and sagittal positions in MNI space, respectively. Cortical network abbreviations are as per Figure 1B.

Right: Quantification (Dice coefficients) of spatial overlap (0=zero overlap; 1=perfect overlap) between the group-level significant thalamic cluster displayed on the left, and each of 9 thalamic nuclear groups derived from a histologically-informed MRI atlas[22] (for detailed description, refer to Methods S1 and Table S2). Thalamic nuclear group abbreviations: Ant=anterior; Md=mediodorsal; aIL=anterior intralaminar; pIL=posterior intralaminar; Pul=pulvinar; VA=ventral anterior; VM=ventromedial; VL=ventrolateral; VP=ventroposterior.

Figure 4 : Thalamic regions in LGS showing abnormally enhanced functional connectivity strength with multiple cortical networks

Upper: Summary image representing thalamic regions showing significantly enhanced connectivity strength (LGS greater than controls, $p<0.05$, 10,000 permutations, corrected for family-wise error following threshold-free cluster enhancement[21]) with multiple cortical networks. The number of cortical networks is given by each thalamic voxel's color (red= enhanced connectivity involving 2 networks; orange=3 networks; yellow=4 networks). Results are displayed on the MNI-152 T1 brain template. The *z* and *x* coordinates on thalamic images indicate the axial and sagittal positions in MNI space, respectively.

Lower: Quantification (Dice coefficients) of spatial overlap (0=zero overlap; 1=perfect overlap) between the group-level thalamic cluster in the upper image, and each of 9 thalamic nuclear groups derived from a histologically-informed MRI atlas[22] (for detailed description, refer to Methods S1 and Table S2). Thalamic nuclear group abbreviations are as per Figure 3.

Supporting information captions

Methods S1: Supplementary methods.

Table S1: Anatomical locations encompassed by cortical networks of interest.

Table S2: Histologically-informed thalamic atlas masks used to assist with identifying thalamic areas of functional connectivity.

Figure S1: Consistency of thalamic parcellations across bootstrapped samples.

Table S3: Dice coefficients quantifying spatial overlap between the winner-takes-all thalamic parcellations (within each group) and the thalamic atlas.

Table S4: Dice coefficients quantifying spatial overlap between regions of significantly positive thalamic connectivity strength (within each group) and the thalamic atlas.

Figure S2: Abnormal thalamocortical functional connectivity strength in lesional and non-lesional LGS sub-groups.

#	Age at study (age at seizure onset), years	Sex	Anti-epileptic medications at time of study	Seizure types	Routine interictal EEG features	Anatomical MRI features	Presumed etiology (*=confirmed neuropathology)	Neuropsychological features (CI=cognitive impairment)
1	25 (0.5)	M	CBZ, LEV, TPM, VPA	Tonic, AA, GTCS	Background slowing, SSW, GPFA	Tuberous sclerosis, multiple lesions	Tuberous sclerosis complex	Severe CI Non-verbal Requires assistance with activities of daily living
2	24 (0.5)	F	LEV, TPM	Tonic, AA, GTCS	Background slowing, SSW, GPFA, bi-frontal discharges	Normal	Unknown	Severe CI Full-scale IQ<40 Lives in supported accommodation
3	41 (1)	F	CBZ, LTG, MDZ, VPA	Tonic, AA, myoclonic, GTCS	Background slowing, SSW, GPFA	Diffuse atrophy	Unknown	Severe CI Non-verbal Lives in supported accommodation
4	25 (2.5)	F	LTG, VPA	Tonic, AA, myoclonic, GTCS	Background slowing, GPFA, SSW, multi-focal discharges	Normal	Chromosome 2q37 deletion	Moderately severe CI Full-scale IQ=40 Lives in supported accommodation
5	35 (2.5)	M	CLB, LTG, TPM, VPA	Tonic, AA, GTCS	Background slowing, SSW, GPFA	Normal	Unknown	Moderately severe CI Minimally verbal Requires assistance with activities of daily living
6	42 (3)	M	LEV, LTG, MDZ	Tonic, AA, GTCS	Background slowing, SSW, GPFA, bi-frontal discharges	L frontal and L temporal pole gliosis	Traumatic brain injury at age 2 years	Moderately severe CI Minimally verbal Lives in supported accommodation
7	14 (4)	M	CBZ, LTG	Tonic, myoclonic, GTCS	SSW, GPFA	Normal	Unknown	Mild impairment in executive function
8	37 (4)	F	CBZ, LEV, LTG, VPA	Tonic, AA, FIAS, GTCS	Background slowing, SSW, GPFA, bi-frontal discharges	Bilateral parietal double cortex	*LIS1* c.484G>A (p.Gly162Ser) gene mutation	Moderate CI Full-scale IQ=60
9	37 (4)	M	CBZ, LEV, TGB	Tonic, AA, FIAS	SSW, GPFA, R temporal/parietal discharges	R temporal cortical loss and gliosis	Peri-natal infarction (*gliosis)	Mild impairment in verbal memory

10	44 (4)	M	CBZ, CLB, LTG, TPM, VPA	Tonic, AA, GTCS	Background slowing, SSW, GPFA, R frontal discharges	L frontal pole gliosis	Unknown	Moderate CI Lives in supported accommodation
11	26 (5)	F	LCM, LTG, PHB, VPA, ZSM	Tonic, AA, FIAS, GTCS	SSW, GPFA, L posterior discharges	Bilateral peri-ventricular nodular heterotopia and polymicrogyria, L posterior schizencephaly	Complex malformation of cortical development	Moderate CI Full-scale IQ=60-63
12	11 (7)	M	CLB, ESX, TPM	Tonic, AA, spasms, GTCS	Background slowing, SSW, GPFA, multi-focal discharges	Unusual L temporal sulcation (incidental)	Unknown	Moderately severe CI Minimally verbal Full-scale IQ=42
13	38 (8)	M	LEV, LTG, TPM, VPA	Tonic, FIAS, GTCS	SSW, GPFA, L frontal discharges	L frontal focal cortical dysplasia	Focal cortical dysplasia (*balloon cells)	Mild impairments in working memory, verbal fluency, psychomotor speed
14	20 (8.5)	M	CBZ, PHT, VPA	Tonic, GTCS	Background slowing, SSW, GPFA	Diffuse atrophy, bilateral peri-ventricular nodular heterotopia	*De novo* chromosome 1q31-3q41 interstitial duplication	Severe CI Non-verbal
15	16 (9)	F	CLB, LEV, STH	Tonic, AA, GTCS	SSW, GPFA, R fronto-temporal discharges	Normal	Unknown	Mild CI Full-scale IQ=70-80 range
16	38 (10)	F	LEV, LTG, OXZ	Tonic, AA, GTCS	Background slowing, SSW, GPFA, R temporal/bi-frontal discharges	Normal	Unknown	Mild impairments in verbal recall, visuospatial processing
17	21 (12)	F	ESX, LTG, PHT	Tonic, AA, GTCS	SSW, GPFA	Normal	Unknown	Unremarkable cognitive profile with schooling difficulties following seizure onset
18	19 (13)	M	LTG, OXZ, PHT, VPA	Tonic, AA, GTCS	Background slowing, SSW, GPFA, bi-frontal discharges	Normal	Chromosome 15q11.2-q13.1 inversion-duplication	Moderate CI Verbal IQ=73 Performance IQ=50
19	18 (16)	F	CBZ, ESX, LEV	Tonic, FIAS	SSW, GPFA, multi-focal	Normal	Acute lymphoblastic	Mild CI

					discharges		leukemia treated with systemic chemotherapy	Full-scale IQ=75-83 range
20	39 (25)	F	CBZ, LTG, PHT, VPA	Tonic, FIAS, GTCS	SSW, GPFA, L frontal discharges	L fronto-temporal cortical loss and gliosis	Traumatic brain injury age 9	Mild CI Full-scale IQ=77

Table 1: Electroclinical characteristics of patients with LGS.

Abbreviations: F=female; M=male; CBZ=carbamazepine; LEV=levetiracetam; TPM=topiramate; VPA=valproate; CLB=clobazam; LTG=lamotrigine; OXZ=oxcarbazepine; ESX=ethosuximide; STH=sulthiame; MDZ=midazolam; TGB=tiagabine; LCM=lacosamide; PHB=phenobarbitone; ZSM=zonisamide; PHT=phenytoin; AA=atypical absence; GTCS=generalized tonic-clonic seizure; FIAS=focal impaired awareness seizure; SSW=slow spike-and-wave; GPFA=generalized paroxysmal fast activity; L=left; R=Right; IQ=intelligence quotient.

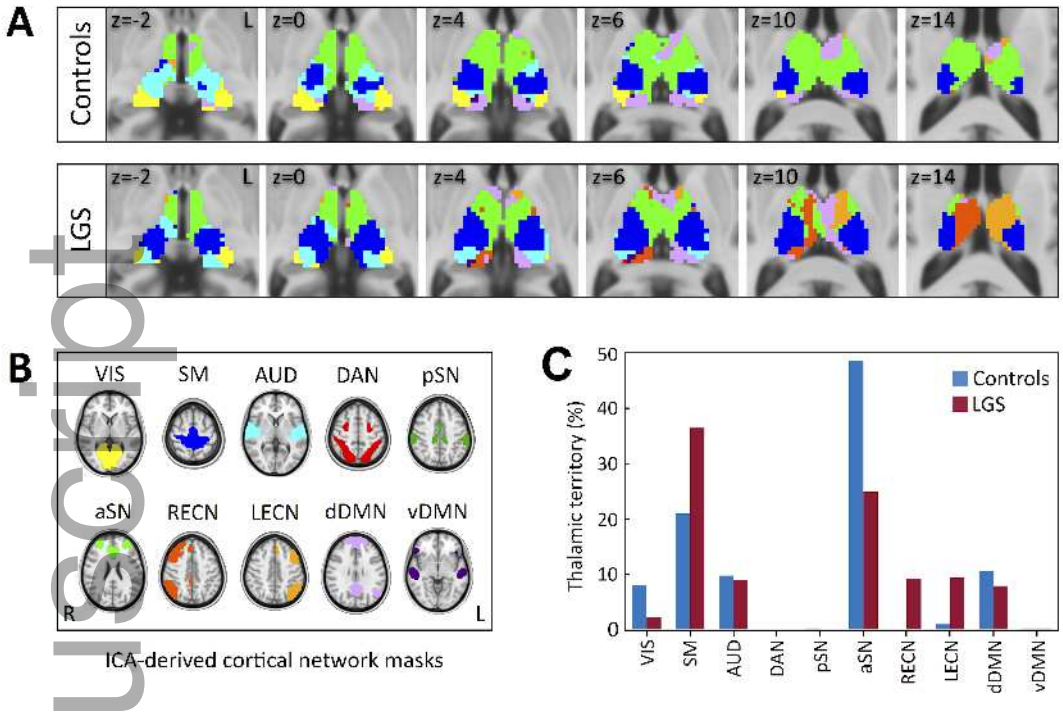

epi_13932_f1.tiff

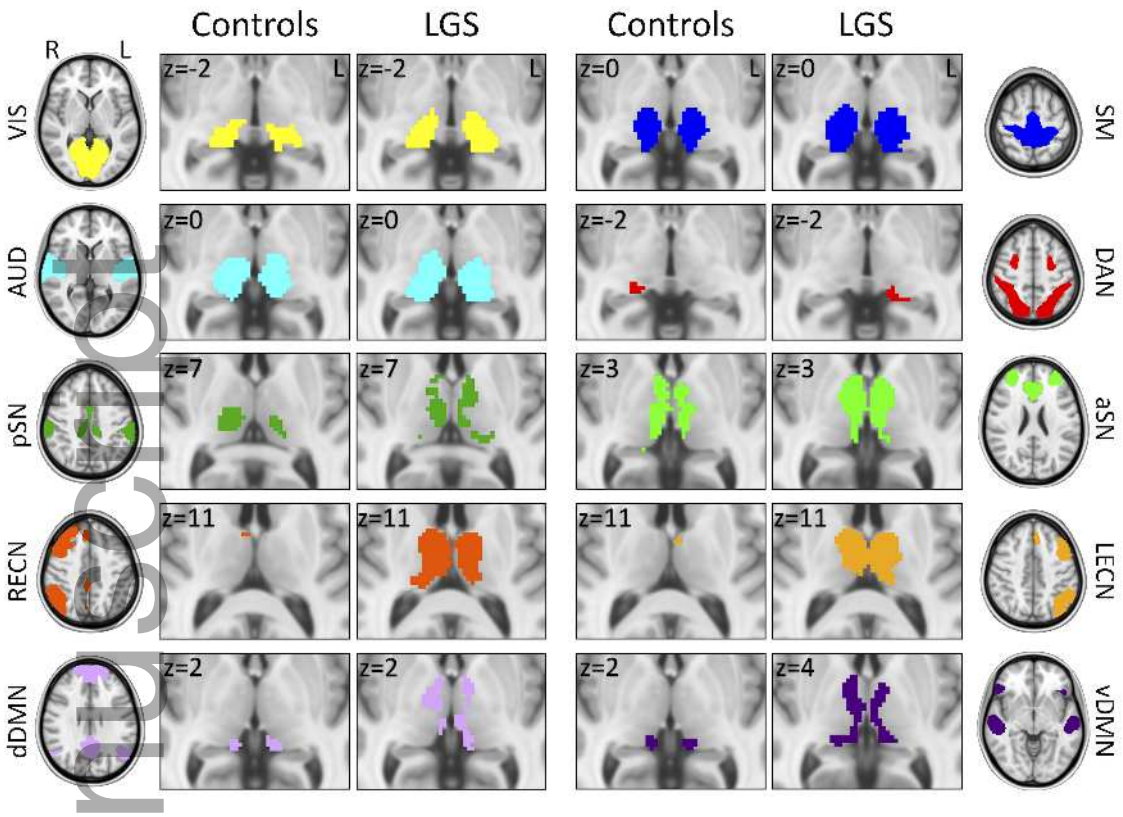

epi_13932_f2.tiff

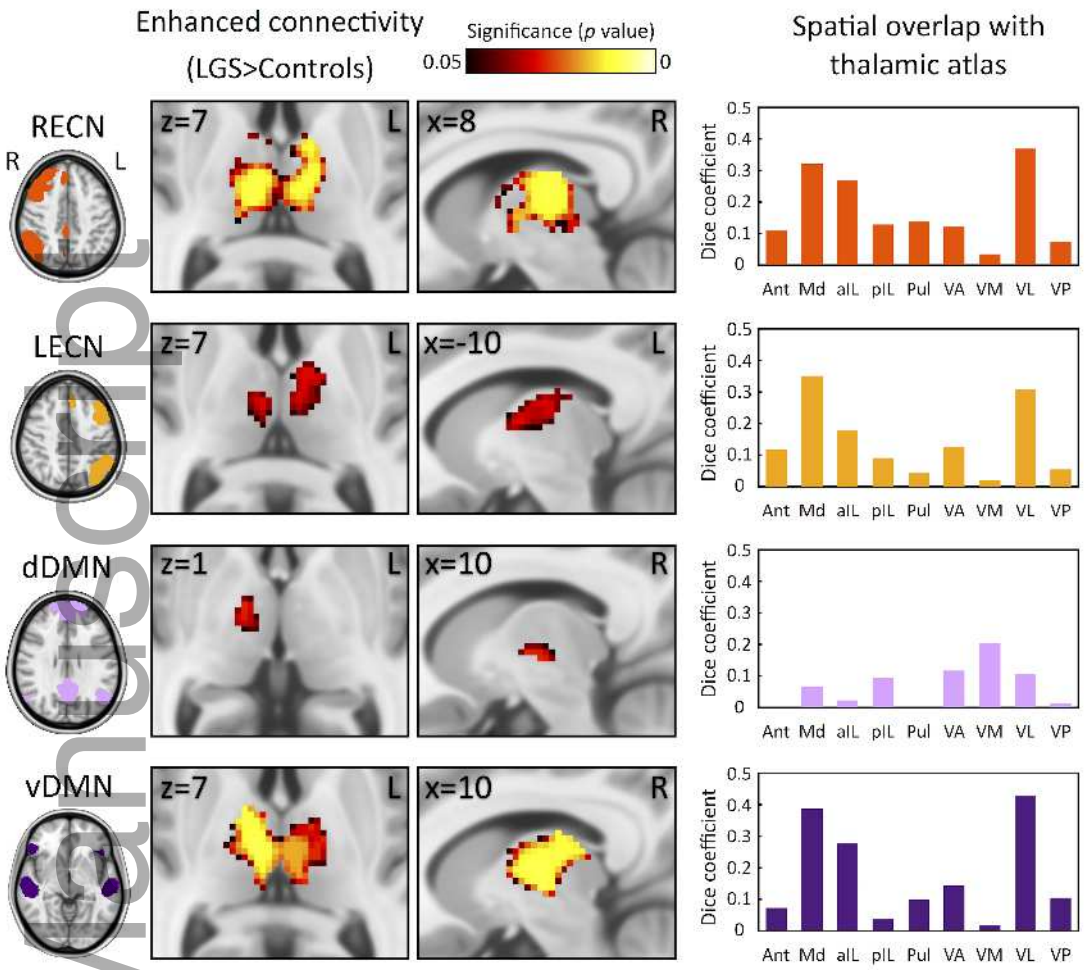

epi_13932_f3.tiff

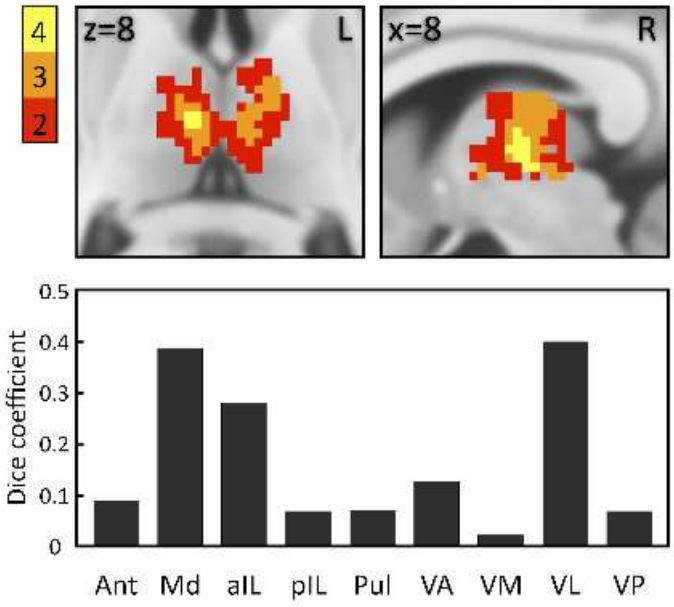

epi_13932_f4.tiff